Electronic Supplementary Information (ESI)

Facile self-assembly of light metal borohydrides with controllable nanostructures

Yongtao Li,[†] Qingan Zhang,[†] Fang Fang,[‡] Yun Song,[‡] Dalin Sun,*[,‡] Liuzhang Ouyang,[§] and Min Zhu*[,§]

[†] School of Materials Science and Engineering, Anhui University of Technology, Maanshan, 243002, China.

[‡] Department of Materials Science, Fudan University, Shanghai, 200433, China.

[§] School of Materials Science and Engineering, South China University of Technology, Guangzhou, 510641, China.

MATERIALS AND METHODS

Materials. HPLC grade tetrahydrofuran (THF) was purchased from Aladdin Reagents (Shanghai) and distilled over drying agents before use. Lithium borohydride ($LiBH_4$, 95%), sodium borohydride ($NaBH_4$, 96%) and calcium borohydride ($Ca(BH_4)_2$, 95%) were purchased from Sigma Aldrich and used without purification. Poly(methyl methacrylate) (PMMA, MW120,000) was purchased from Alfa Aesar.

Synthesis of Borohydride NPs. PMMA-capped borohydrides NPs were synthesized via an EISA method. All sample procedures were carried out in an Ar-filled glovebox equipped with a circulative purification system. In a typical synthesis procedure, borohydrides and PMMA were individually dissolved in THF with stirring vigorously until

the solution became transparence. Then 10 ml of the borohydrides/THF solution was added dropwise to a solution of PMMA (100 mg) in 10 ml of THF and stirred vigorously for 2 h to obtain a homogeneous solution. Finally, the solutions were maintained at ambient conditions for self-assembly and were dried upon self-evaporation of THF with a velocity of about 1.34×10^{-4} g/s (the evaporation area of 12.56 cm^2).

Synthesis of Size-altered $LiBH_4$ NPs via Changing the Concentration. Varying amounts of $LiBH_4$ solution in 10 ml of THF were added (ranging from 1 mmol to 5 mmol). Then the $LiBH_4$/THF solution was added dropwise over a period of 20 minutes into a solution of PMMA (100 mg) in 10 ml of THF, stirred vigorously for 2 h and maintained at ambient conditions for self-assembly which was induced by the self-evaporation of THF.

Characterization. To reveal the phase components and structure, XRD was carried out on a Rigaku D/max 2400 with Cu Ka radiation at 50 kV and 30 mA. FTIR spectroscopy was carried out to examine chemical bond variations on a PerkinElmer FTIR 1710 spectrometer. To examine the microstructural and elemental composition, TEM observations were carried out on a JEOL JEM-2100F which was equipped with an EDX spectrometer For TEM measurements, samples were prepared by placing a drop of solution on a porous carbon film supported on a copper grid which allowed the solvent to evaporate in an Ar atmosphere. The evolved hydrogen gas process was analyzed using a Netzsch STA 409 PC analyzer equipped with a QMS 403C mass spectrometer at a ramping rate of 10 ºC/min under a flowing Ar (99.999% purity) atmosphere. A stability test was performed by exposing the samples to the atmosphere with 60% relative humidity, and the photographic changes and weight increase were examined using a CANON camera and an electronic balance, respectively.

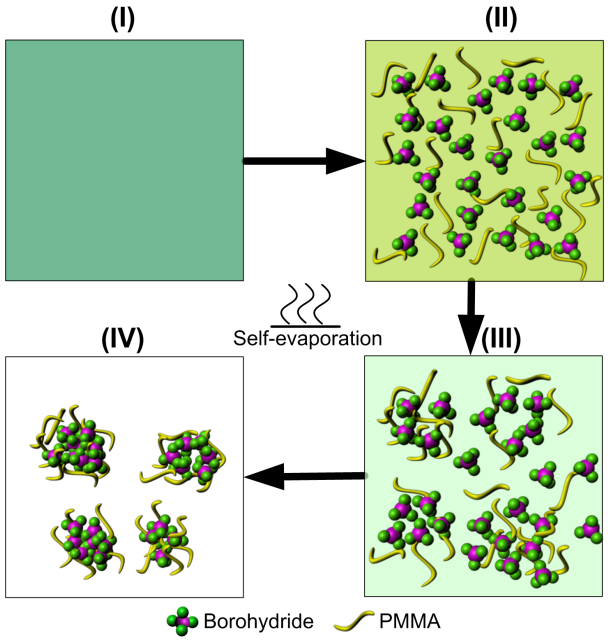

Fig. S1. A plausible mechanism for the formation of dispersed borohydride NPs capped by PMMA. (I) Both borohydride and PMMA dissolve in volatile THF to form a homogeneous solution; (II) upon self-evaporation of THF, the supersaturated borohydride recrystallizes into small clusters along with in-situ adsorption and precipitation of PMMA; (III) the borohydride clusters tend to aggregate and grow along with continued precipitation and self-assembly; (IV) with the completion of evaporation and phase separation, the precipitated PMMA converts to a polymer matrix in which facilitates the embedding of borohydride NPs.

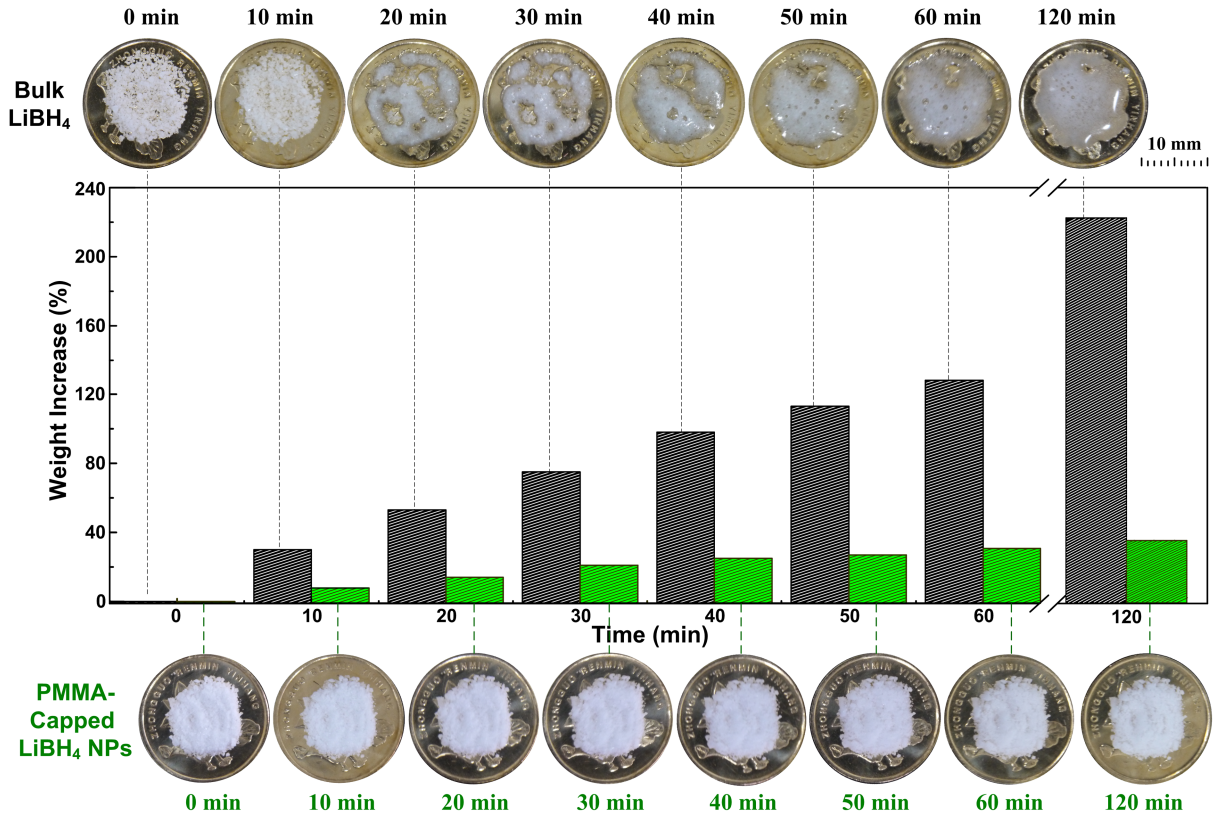

Fig. S2. Photographs and the relative weight increase of bulk $LiBH_4$ and PMMA-capped $LiBH_4$ NPs that were set on a copper surface during atmospheric exposure with 60% relative humidity.

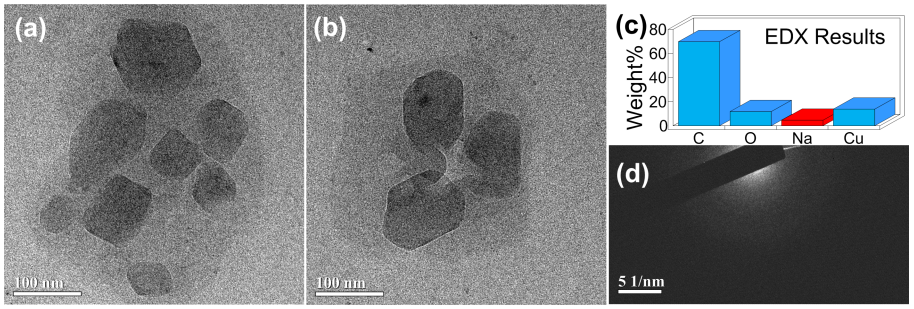

Fig. S3. (a, b) TEM images, (c) elemental EDX spectroscopy analysis and (d) SAED patterns for polygon $NaBH_4$ NPs.

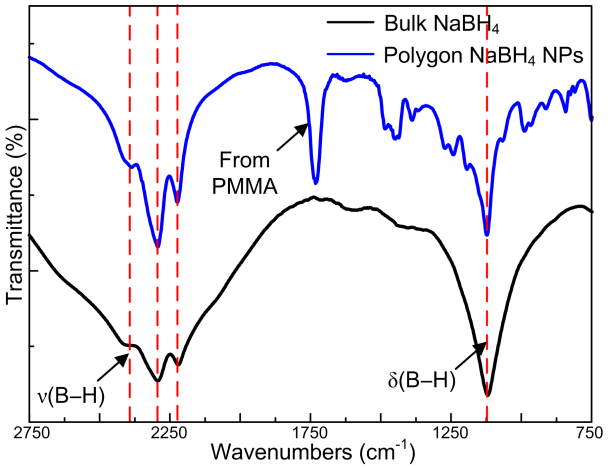

Fig. S4. FTIR spectra for polygon $NaBH_4$ NPs and bulk $NaBH_4$.

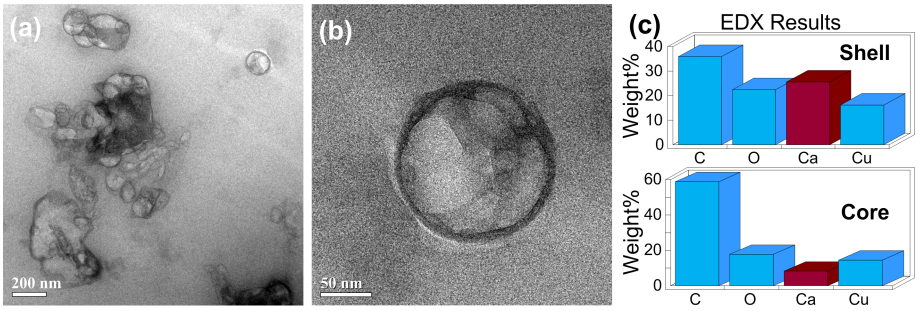

Fig. S5. (a, b) TEM images and (c) elemental EDX spectroscopy analysis for hollow $Ca(BH_4)_2$ NPs.

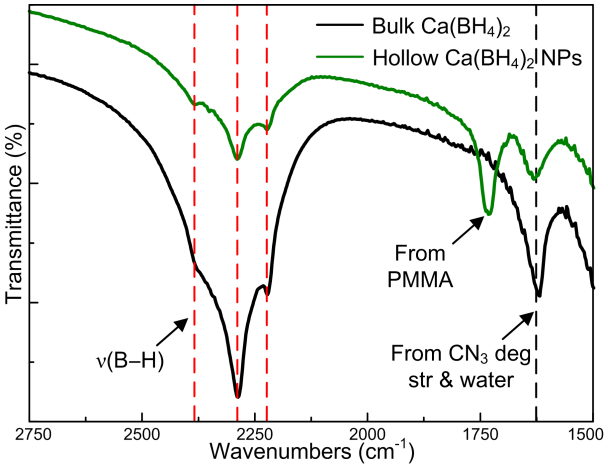

Fig. S6. FTIR spectra for hollow $Ca(BH_4)_2$ NPs and bulk $Ca(BH_4)_2$.